Molecular Modeling and Mutagenesis Reveals a Tetradentate Binding Site for Zn^{2+} in $GABA_A$ $\alpha\beta$ Receptors and Provides a Structural Basis for the Modulating Effect of the γ Subunit

James R. Trudell,*,† Minerva E. Yue,‡ Edward J. Bertaccini,† Andrew Jenkins,§ and Neil L. Harrison‡

Department of Anesthesia, Stanford University School of Medicine, Stanford, California 94305-5117, Department of Anesthesiology, Weill Medical College of Cornell University, New York, New York, and Department of Anesthesiology, Emory University School of Medicine, Atlanta, Georgia

Received August 30, 2007

Gamma-aminobutyric acid type A receptors ($GABA_A$-R) containing $\alpha1\beta2\gamma2$ subunits are weakly inhibited by Zn^{2+}, whereas receptors containing only the $\alpha1\beta2$ subunits are strongly inhibited. We built homology models of the ion pores of $\alpha1\beta2$ and $\alpha1\beta2\gamma2$ $GABA_A$-R using coordinates of the nicotinic acetylcholine receptor as a template. Threading the $GABA_A$-R $\beta2$ sequence onto this template placed the 17′ histidine and the 20′ glutamate residues at adjacent locations in the mouth of the pore, such that a nearly ideal tetradentate site for Zn^{2+} was formed from two histidine and two glutamate residues between adjacent β subunits in the $\alpha1\beta2$ $GABA_A$-R. Following optimization with CHARMM, the distance between the α-carbons of the adjacent histidine residues was approximately 9.2 Å, close to the ideal distance for a Zn^{2+} binding site. Loss of inhibition by Zn^{2+} in $\alpha1\beta2\gamma2$ $GABA_A$-R can be explained by the geometry of these residues in the arrangement $\alpha1\beta2\gamma2\alpha1\beta2$, in which the nearest C-α-C-α distance between the histidine residues is 15.5 Å, too far apart for an energetically optimal Zn^{2+} binding site. We then mutated the γ subunit at the 17′ and/or 20′ positions. Zn^{2+} inhibition was not restored in $\alpha1\beta2\gamma2$ (I282H) receptors. A novel finding is that the modeling shows the native 20′ lysine in $\gamma2$ can compete with Zn^{2+} for binding to the inserted 17′ histidine. Sensitivity to Zn^{2+} was restored in the double mutant receptor, $\alpha1\beta2\gamma2$ (I282H; K285E), in which the competition with lysine was removed and a more favorable Zn^{2+} binding site was formed.

INTRODUCTION

Gamma-aminobutyric acid type A receptors ($GABA_A$-R) are members of the Cys-loop superfamily of ligand-gated ion channels (LGICs) that includes nicotinic acetylcholine (nAChR) and glycine receptors (Gly-R). Functional $GABA_A$-Rs are formed as pentameric combinations of polypeptide subunits. Multiple subunit isoforms exist, which can potentially give rise to a large number of receptor variants,[1] although few of these exist naturally in the brain.[2] In fact, the vast majority of neuronal $GABA_A$-R occur at synapses as $\alpha\beta\gamma$ combinations or extrasynaptically as $\alpha\beta\delta$ combinations.[3] A smaller proportion may exist as $\alpha\beta$ combinations.[4]

Zn^{2+} interacts with many ion channels[5] and functions as an endogenous modulator of neuronal excitability via its effects on LGICs such as NMDA receptors and voltage-gated K^+ channels.[5,6] Zn^{2+} can therefore regulate synaptic transmission and plasticity.[7] $GABA_A$ $\alpha\beta$ receptors are inhibited by low (≤ 1 μM) concentrations of Zn^{2+},[5,8−10] but the affinity of Zn^{2+} as an inhibitor is greatly reduced (50−3000-fold) in $GABA_A$-R incorporating γ subunits.[1,9,11,12] Indeed, this property is so distinct that it has been widely used to document functional expression of the γ subunit in recombinant $GABA_A$-R.[9,13]

Although there are multiple Zn^{2+} binding sites on $GABA_A$ $\alpha\beta$ receptors, mutagenesis experiments have identified the 17′ residue histidine 267 in the second transmembrane segment (TM2) of the β subunit as being principally involved in the highest affinity Zn^{2+} binding site in these receptors.[12,14,15] This histidine residue lies external to the gate and selectivity filter in these $\alpha\beta$ receptors. Up to now, the lack of Zn^{2+} binding affinity in the $\alpha\beta\gamma$ $GABA_A$ receptors has not been satisfactorily explained, despite the presence of a 17′ isoleucine in TM2 of the γ subunit instead of the histidine found at the homologous position in the β subunit. We noticed that there was an additional difference in sequence at the 20′ position in TM2 between the β subunit (which has glutamate at this position) and the γ subunit (which has lysine). We therefore investigated the role of the glutamate residue at the 20′ position using a combination of site-directed mutagenesis and molecular modeling. Our results show clearly that a 20′ lysine destabilizes the binding of Zn^{2+} to the $\alpha\beta\gamma$ receptor and that replacement of the lysine with glutamate increases the affinity of Zn^{2+} binding. Molecular modeling of $GABA_A$ $\alpha\beta$ receptors shows that the adjacent 17′ histidine and 20′ glutamate can form a tetradentate Zn^{2+} binding site of ideal geometry, which is disrupted by the presence of a 20′ lysine in the γ subunit.

METHODS

Molecular Modeling. There is now a general consensus that the pore regions are structurally conserved among the

* Corresponding author phone: (650)725 5839; e-mail: trudell@stanford.edu.
† Stanford University School of Medicine.
‡ Weill Medical College of Cornell University.
§ Emory University School of Medicine.

10.1021/ci700324a CCC: $40.75
Published on Web 01/16/2008

Cys-loop LGICs.[4,16−20] This conservation of structure is supported by sequence alignments[4,16] and the ability to make functional channels from chimeric subunits, e.g., between $GABA_A$-R and Gly-R subunits[21] or 5-HT3A and nAChR subunits.[22]

The near atomic resolution structure (approximately 2 Å) of the acetylcholine binding protein (AChBP) of *Lymnaea stagnalis*[23] has been used as a template for fitting the electron density maps from cyroelectron microscopy of the nAChR. This has resulted in models for the extracellular domain of the nAChR and other LGICs.[19,24] We used a structural model of the pore region based on the latest of these structures (PDB ID 2BG9, approximately 4 Å resolution). The ion pore in 2BG9 is formed from five α-helical transmembrane segments 2 (TM2), and this structure was used as a template for modeling the binding of Zn^{2+} to $GABA_A$-R in the present study. Since the numbering of amino acid residues varies greatly between members of the Cys-loop superfamily, the residues in TM2 of the $GABA_A$-R subunits are referred to here using the prime nomenclature (1′ to 20′), corresponding to residues Met243 to Glu262 in the *Torpedo* nAChR α subunit.

We edited the most recent cryoelectron structure of the nAChR (PDB ID 2BG9)[19] to provide a template for the $GABA_A$-R models. The coordinates provided a model of the TM2 α-helices that line the pore of the nAChR ion channel. The channel-lining His267 residues in $GABA_A$-R β2 subunits that are involved in Zn^{2+} binding align with the 17′ Val259 in nAChR α subunits.[16] We used the Homology module of Insight II 2005L (Accelrys, San Diego, CA) to thread $GABA_A$-R residues into the TM2 α-helices of nAChR (PDB ID 2BG9; models α1β2, Figure 1A,B and models α1β2γ2s, Figure 1C,D). We added hydrogen atoms and adjusted partial atomic charges of ionizable groups to correspond to pH 7.0. We used the autorotamer function of the Biopolymer module of Insight 2005L to find the optimum side-chain rotamers. We measured the C-α-to-C-α distance between histidine residues in each model. Before starting optimization with the CHARMM module of Insight 2005L, we built several starting 'poses' by manually adjusted the dihedral angles of the side chains of adjacent histidine residues in model α1β1 to obtain a close NE2-to-NE2 distance. We used the NE2 (ϵ tautomer) forms of histidine because it is the most common form in crystal structures that feature high affinity Zn^{2+} binding sites.[25] We built a Zn^{2+} atom in the CHARMM force field (Accelrys, San Diego, CA), assigned the MZN potential functions to it, and inserted it at different positions between these side chains to form a set of starting poses. At this point, the histidine C-α-to-C-α distance was 9.2 Å, the partial atomic charges of both histidine NE2 atoms were −0.40, and the Zn^{2+} atom formal charge was + 2.0. We tethered all backbone atoms of the models to their coordinates in 2BG9 with a harmonic force constant of 1000 kcal/A^2 and then optimized the structures to a derivative of 0.001 kcal/A with the CHARMM module of Insight 2005L using a fixed dielectric of 1 and a smooth electrostatic cutoff at 15 Å.

Model of α1β2 $GABA_A$-R. In the case of $GABA_A$-R α1β2, optimization of the models produced dimensions close to those of an ideal Zn^{2+} binding site (the NE2-to-NE2 distance between adjacent 17′ histidines was 4.63 Å, Figure 1A). We performed further tests to be sure that this was a robust result: First, we tried different poses of the histidine side chain torsion angles and the starting position of the Zn^{2+} atom between the histidine NE2 atoms. Second, we subjected the optimized model to 10 000 steps of molecular dynamics in CHARMM at 300 K, in the NVT ensemble (constant number of atoms, volume, and temperature), with the same backbone restraints as above. We then reoptimized the structure as described above. The model showed that the two 17′ histidine and the two 20′ glutamate residues could form a tetradentate Zn^{2+} binding site of nearly ideal geometry (Figure 1B), although during the molecular dynamics simulation the structure was fluid and frequently one residue moved away from the Zn^{2+} atom. We then tested the effect of hydration of the ion pore by solvating the pentameric bundle plus the Zn^{2+} atom (as optimized above) with a 5 Å layer of water using the default solvation algorithm of Insight II 2005L. We tethered all backbone atoms of the models to their coordinates in 2BG9 with a harmonic force constant of 1000 kcal/A^2 and then optimized the structures to a derivative of 0.001 kcal/A with the CHARMM module of Insight 2005L using a fixed dielectric of 1 and a smooth electrostatic cutoff at 15 Å. We subjected the optimized model to 10 000 steps of molecular dynamics in CHARMM at 300 K, in the NVT ensemble with the same backbone restraints as above (Figure 1B).

We built a similar model of $GABA_A$-R α1β2γ2 (Figure 1C,D), an additional model incorporating the 17′ isoleucine to histidine mutation in the γsubunit of α1β2γ2, and a model of α1β2γ2, in which the γ subunit had both the 17′ isoleucine to histidine and 20′ lysine to glutamate mutations. A novel finding of the present study was that the model of $GABA_A$-R α1β2γ2s with only the (I282H) mutation would not provide a good binding site for Zn^{2+} because the remaining 20′ lysine side chain could interact with neighboring negatively charged side chains (similar to the lysine interaction in Figure 1C,D). In contrast, the model of $GABA_A$-R α1β2γ2s (I282H; K285E) could provide a good Zn^{2+} binding site (similar to that formed from adjacent β subunits in Figure 1A). These predictions were tested experimentally as described below.

Mutagenesis and Expression in HEK Cells. The cDNA encoding the $GABA_A$-R α1, β2, and γ2s subunits were subcloned into the pCIS2 and pcDNA3.1+ expression vectors. Site-directed mutagenesis was performed using the QuikChange method as described (Stratagene, La Jolla, CA), and mutant clones were confirmed through automated fluorescent DNA sequencing (Biotechnology Resource Center, Cornell University). Wild-type or mutant receptor cDNA was transiently expressed in human embryonic kidney (HEK) 293 cells (American Type Culture Collection, Rockville, MD). For electrophysiological recordings, cells were plated onto glass coverslips coated with poly-D-lysine (Sigma) and transfected with 2.5 μg of each cDNA plasmid using the calcium phosphate precipitation method. Cells were washed after 24 h of contact with cDNA precipitate and used for patch-clamp recording 48−72 h post transfection. The five constructs tested were as follows: [1] α1β2, [2] α1β2γ2, [3] α1β2γ2(I282H), [4] α1β2γ2(I282H; K285A), and [5] α1β2γ2(I282H; K285E).

Electrophysiology. GABA currents were recorded at room temperature (22 °C) using the whole cell patch-clamp method (voltage clamped at −60 mV) using an Axopatch 200 amplifier (Molecular Devices, Foster City, CA). The extracellular solution contained (in mM) 145 NaCl, 3 KCl, 1.5

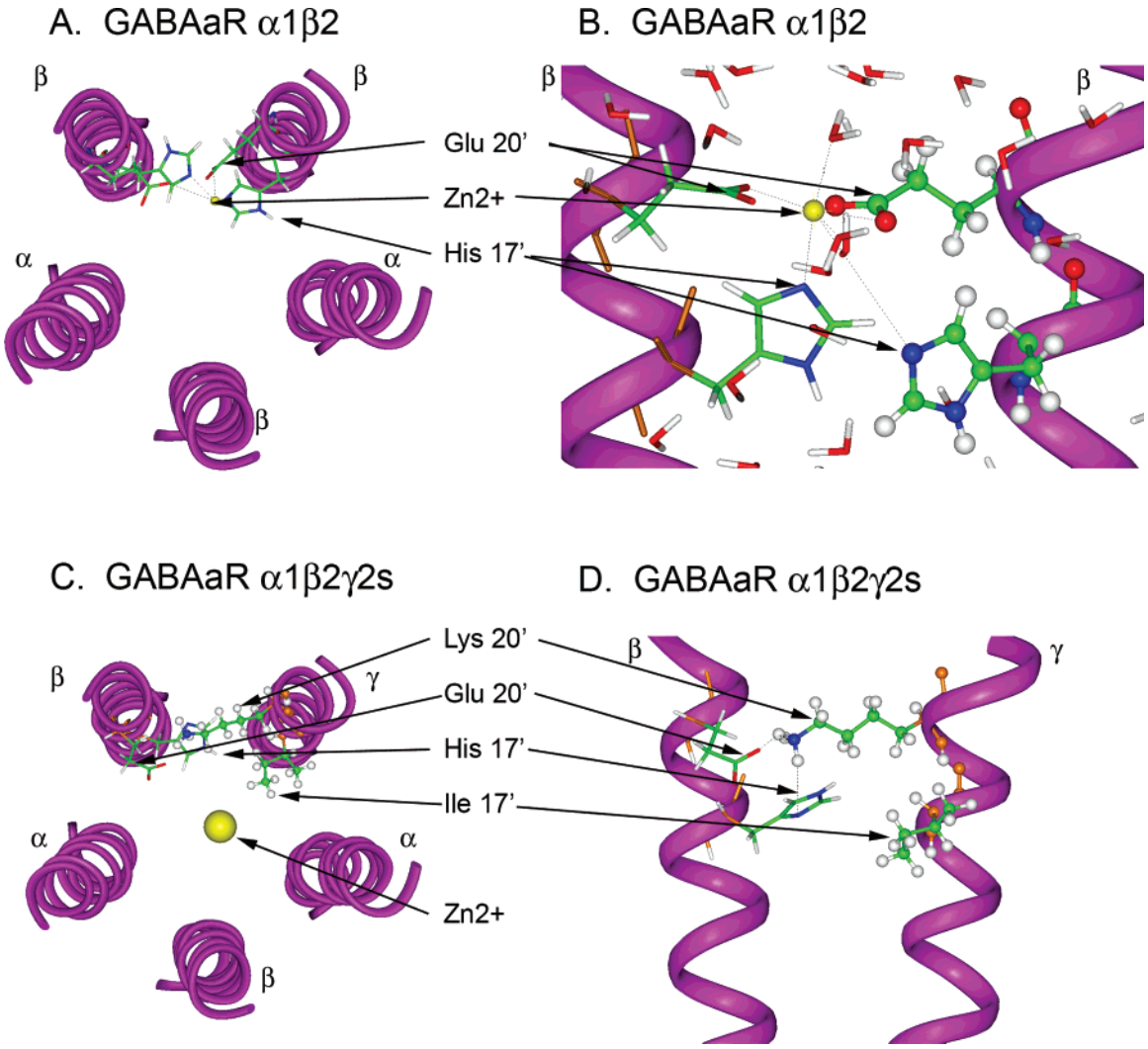

Figure 1. (A) A model of $GABA_A$-R α1β2 with Zn^{2+} bound in a tetradentate binding site composed of two histidine and two glutamate residues. The model is viewed from the extracellular side along the axis of the ion pore. Residues at positions 17′ and 20′ are rendered as stick figures and the atoms are as follows: carbon (green), oxygen (red), nitrogen (blue), hydrogen (white), and Zn^{2+} (yellow). The backbones of the transmembrane α helices (TM2) are shown as violet tubes (for scale, they are 25 Å long), and dotted lines indicate selected hydrogen bonds. A model (not shown) of $GABA_A$-R α1β2γ2s (I282H; K285E) provides an essentially identical starting structure. (B) A side view of the same model of $GABA_A$-R α1β2 as in (A) but after hydration, optimization, and molecular dynamics simulation (as described in Methods). This model is viewed along the plane of the membrane from the center of the ion pore and is zoomed in. For clarity, only the two GABAa-R β2 subunits of interest are shown, and the residues of the right TM2 are rendered as ball and stick. The right-hand 17′ histidine has moved away from the Zn^{2+}, and two water molecules have taken its place. (C) A model of GABAa-R α1β2γ2s with a γ2s subunit interposed between two β2 subunits. The model is viewed from the extracellular side along the axis of the ion pore. The Zn^{2+} was manually placed on the ion pore axis and was rendered in full van der Waals diameter to indicate its relative size. The Zn^2 did not move to a consistent binding position during optimizations with CHARMM. (D) A side view of the same model of GABAaR α1β2γ2s as in (C) but viewed along the plane of the membrane from the center of the ion pore and zoomed in. This view clearly shows that the 20′ lysine side chain of the γ2s subunit (rendered in ball and stick) can bind to both the 17′ histidine and the 20′ glutamate residues in the β2 subunit (rendered in stick).

$CaCl_2$, 1 $MgCl_2$, 6 D-glucose, and 10 HEPES, pH adjusted to 7.4 with NaOH. Patch pipettes had a resistance of 5 MΩ when filled with the intracellular solution, which contained (in mM) 145 *N*-methyl-D-glucamine hydrochloride, 0.1 $CaCl_2$, 5 dipotassium ATP, 1.1 EGTA, 2 $MgCl_2$, and 5 HEPES, pH adjusted to 7.2 with KOH. GABA or $ZnCl_2$ were rapidly applied (~50 ms exchange time) to the cell via a multichannel infusion pump and motor-driven solution exchange device (Rapid Solution Changer RSC-100; Molecular Kinetics, Pullman, WA).

The peak current amplitude of each agonist response was measured for each cell, and the agonist concentration−response amplitude data were fitted using a sum of least-squares method to a Hill equation of the form $I = I_{MAX} \times [\text{agonist}]^{n_H}/([\text{agonist}]^{n_H} + EC_{50}^{n_H})$, where I is the peak current, I_{MAX} is the maximum whole cell current amplitude, [agonist] is the agonist concentration, EC_{50} is the agonist concentration eliciting a half-maximal current response, and n_H is the Hill coefficient. The concentration dependence of the inhibition of the GABA-induced currents by Zn^{2+} was fit with the Hill equation, $I = I_{MAX} \times [Zn^{2+}]^{n_H}/([Zn^{2+}]^{n_H} + IC_{50}^{n_H})$, [where $[Zn^{2+}]$ is the Zn^{2+} concentration and IC_{50} is the concentration of Zn^{2+} that elicits half-maximal inhibition], using Prism 4.0 (GraphPad, San Diego, CA).

All working solutions of $ZnCl_2$ were prepared daily in double-distilled water by diluting a stock solution. In all experiments, GABA was applied at an EC_{50} concentration

appropriate for the mutant or wild-type $GABA_A$-R under study. To determine the IC_{50} value for Zn^{2+}, a series of progressively increasing Zn^{2+} concentrations was applied to the cell.

RESULTS

Results and Predictions from Modeling. In the present study, we used molecular modeling to test the hypothesis that histidine and glutamate residues at the 17′ and 20′ positions in adjacent TM2 α-helices of α1β2 $GABA_A$-R provide high affinity Zn^{2+} binding sites and that these sites are disrupted when a γ subunit replaces one of the adjacent β subunits in α1β2γ2 $GABA_A$-R. We used a variety of published information to allow us to validate our molecular models by comparison with known structures of high affinity Zn^{2+} binding sites. Analysis of 111 structures of Zn^{2+} binding proteins, all available in the Protein Data Bank (PDB),[25] as well as data on the protein engineering of Zn^{2+} binding sites[26] provided us with the following criteria: (1) The ideal C-α-to-C-α distance between histidine residues should be <13 Å; (2) Any of the five histidine side chain rotational conformers are acceptable; (3) The histidine NE2-to of Zn^{2+} distance should be <2.1 Å; and (4) The ideal histidine NE2-to-Zn2+-to-histidine NE2 angle should be about 102°.

We built and optimized molecular models of the $GABA_A$-R ion pore in which Zn^{2+} was bound between 17′ histidine and 20′ glutamate residues in adjacent TM2 α-helices (from α and β subunits) and then repeated this in models in which one of the adjacent β subunits was replaced by a γ subunit. We found that the latter arrangement could not provide a high affinity Zn^{2+} binding site.

The results of this study were clear: model α1β2 (Figure 1A) provided an excellent tetradentate of Zn^{2+} binding site. Model α1β2 satisfied the four criteria listed above very well. Following optimization with the CHARMM module, the C-α-to-C-α distance between histidine residues was 9.2 Å, the histidine side-chain rotational conformers were acceptable, the histidine NE2-to of Zn^{2+} distances were both 2.04 Å, and the histidine NE2-to-Zn^{2+}-to-histidine NE2 angle was 114°. Using different starting poses, including changing histidine side-chain rotamers, moving the Zn^{2+} atom off the histidine NE2 to histidine NE2 centerline, and performing restrained molecular dynamics typically resulted in three of the possible four residues bound to Zn^{2+}. When a typical assembly was hydrated with explicit waters, optimized, and simulated with molecular dynamics at 300 K, one or two water molecules bound to Zn^{2+} and also formed hydrogen bonds with nearby histidine or glutamate residues (Figure 1B). Similar coordination geometries have been found in crystal structures of Zn^{2+} binding proteins and were termed a "water-elec-His-Zn motif".[25]

In contrast, model α1β2γ2 (Figure 1C), with a γ subunit substituted for one of the adjacent βsubunits, did not provide a good binding site for Zn^{2+}. This was expected as the C-α-to-C-α distance between histidine residues on the separated β subunits was now 15.5 Å, greater than the maximum of <13 Å found in PDB crystal structures.[25] It would seem that the Zn^{2+} atom could still bind between one 17′ histidine NE2 atom and one 20′ glutamate. However, as described below, this was not the case because the potential bidentate site on an adjacent β subunit was partially blocked by the 20′ lysine residue on the neighboring γ subunit.

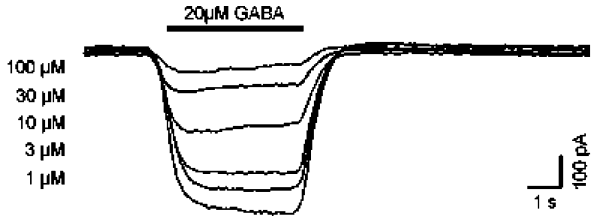

Figure 2. Representative electrophysiological recording of GABA-induced Cl^- current recorded at human embryonic kidney 293 cell expressing α1β2 receptors in the presence of a varying concentration of $ZnCl_2$.

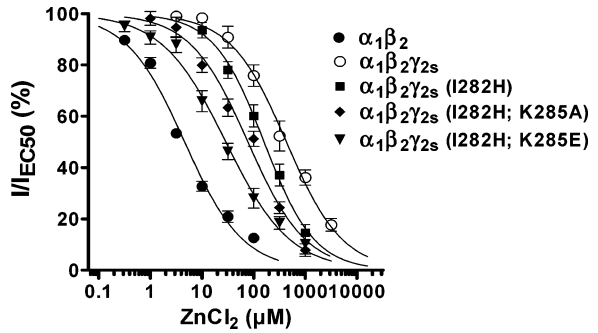

Figure 3. Concentration−response curves for Zn^{2+} inhibition of recombinant $GABA_A$ α1β2γ2 wild-type and mutant receptors. Zn^{2+} current responses are normalized to the GABA EC_{50} current amplitude. The normalized data were fitted by a Hill equation. Data points are shown as a mean of at least 15 cells, and error bars indicate standard errors.

The most surprising result was predicted from the model of the 17′ mutation α1β2γ2(I282H) (similar to the lysine charge pair interaction in Figure 1C). Even when the 17′ histidine is substituted into the γ subunit, it did not provide a high affinity tridentate binding site for Zn^{2+} because the positive amino end of the 20′ lysine side chain was able to approach the negative NE2 nitrogen of the histidine side chain and form an ion pair. Alternatively, the 20′ lysine side chain could form an ion pair with the 20′ glutamate residue on the adjacent β subunit. As expected, the model α1β2γ2 (I282H; K285E) (similar to the binding site in Figure 1A) does exhibit a satisfactory tetradentate binding site for Zn^{2+}. The experimental investigation of these theoretical predictions is described below.

Results from Site-Directed Mutagenesis and Expression of $GABA_A$-R. We measured Zn^{2+} inhibition of $GABA_A$-R experimentally by recording GABA-induced Cl^- current in human embryonic kidney (HEK 293) cells expressing recombinant $GABA_A$-R. We first expressed α1β2 $GABA_A$-R and activated these receptors in the presence of varying concentrations of Zn^2 (Figure 2). We then constructed concentration−response curves for Zn^{2+} inhibition in wild-type and a series of mutant α1β2γ2 $GABA_A$-Rs (Figure 3). The results of this study are summarized in Figure 4, in which the IC_{50} concentrations are displayed for Zn^{2+} inhibition of each wild-type and mutant $GABA_A$-R. Table 1 lists maximal current, GABA EC_{50} values, and Hill coefficients for each receptor as well as the IC_{50} responses and Hill coefficients for inhibition by Zn^{2+}. We emphasize that, in the present study, we are mainly concerned with left and right shifts in the EC_{50} values for inhibition by Zn.[2] These responses of a large population of identical receptors give a good statistical average of the response to binding of Zn.[2] In contrast, changes in I_{MAX} values given in Table 1 using the whole

Table 1. Summary of GABA Activation and Zn^{2+} Inhibition of Cl^- Currents for Recombinant $\alpha1\beta2$ and $\alpha1\beta2\gamma2s$ Wild-Type and Mutant Receptors

	GABA activation				Zn^{2+} inhibition		
	I_{MAX} (pA)	EC_{50} (μM)	n_H	N	IC_{50} (μM)	n_H	N
$\alpha_1\beta_2$	960.1 ± 122.8	14.0 ± 3.3	1.1 ± 0.1	10	4.0 ± 0.4	0.9 ± 0.1	19
$\alpha_1\beta_2\gamma_{2s}$	1636.9 ± 224.8	27.8 ± 4.1	1.2 ± 0.1	15	354.9 ± 63.5	0.8 ± 0.1	17
$\alpha_1\beta_2\gamma_{2s}$(I282H)	1732.5 ± 309.4	24.8 ± 4.2	1.0 ± 0.1	14	194.7 ± 35.6	1.0 ± 0.1	15
$\alpha_1\beta_2\gamma_{2s}$(I282H; K285A)	1112.2 ± 329.2	21.1 ± 5.9	1.0 ± 0.1	10	85.1 ± 10.3	0.9 ± 0.1	15
$\alpha_1\beta_2\gamma_{2s}$(I282H; K285E)	1083.6 ± 157.1	25.2 ± 2.9	0.8 ± 0.1	17	26.2 ± 3.2	0.9 ± 0.1	15

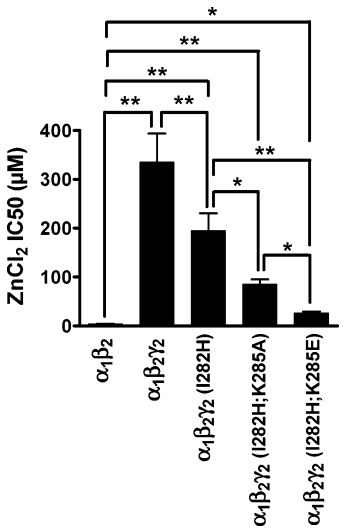

Figure 4. Zn^{2+} IC50 concentrations for each subunit combination. The mean concentration value is shown for each receptor subtype with the error bars representing standard errors. Statistical significance was assessed using a one-way ANOVA with Dunnett's Multiple Comparison Post Test. (* $P < 0.05$; ** $P < 0.01$).

cell patch-clamp method could be a result of differences in receptor expression or in ion channel conductance. In the present study, they indicate that expression was normal and that the population was large enough for reliable measurement of shifts in the EC_{50} values for inhibition by Zn.[2]

As expected, and as previously reported, we observed a dramatic increase in Zn^{2+} IC_{50} between $\alpha1\beta2$ and $\alpha1\beta2\gamma2$ $GABA_A$-Rs. This increase was only partially reversed in the $\alpha1\beta2\gamma2$ (I282H) mutant. Our hypothesis was that this is because the 20′ lysine is able to compete with Zn^{2+} for the binding site. In these experiments we also tested an additional double mutation that was not studied with molecular modeling - $\alpha1\beta2\gamma2$ (I282H; K285A). The response of this mutant to Zn^{2+} (better than $\alpha1\beta2\gamma2$ $GABA_A$-R but not as good as $\alpha1\beta2$ $GABA_A$-R) confirmed that the 20′ lysine side chain made an important reduction in binding affinity, presumably by blocking the binding of Zn^{2+} to the NE2 nitrogen of His282 or the carboxylate oxygen of Glu285. This hypothesis was supported by the decrease in IC_{50} for Zn^{2+} observed in the double mutant $\alpha1\beta2\gamma2$ (I282H; K285A) $GABA_A$-R, in which the proposed interaction between the lysine and histidine side chains was removed.

DISCUSSION

This combined modeling and mutagenesis study helps to explain and refine the molecular basis for previous experimental observations of inhibition of $\alpha1\beta2$ $GABA_A$-R by low concentrations of Zn^{2+}.[5,9,12,14,15] The results support previous models of subunit composition in $\alpha1\beta2\gamma2$ $GABA_A$-R[4,27,28] and the relative clockwise ordering of subunits (viewed from the extracellular side) as $\alpha1\beta2\gamma2\alpha1\beta2$.[27]

The addition of a γ subunit to $\alpha1\beta2$ $GABA_A$-R has been reported to increase the IC_{50} for inhibition by Zn^{2+} by between 50- and 3000-fold.[1,9,11,12,14,15] Of course, this wide range of ratios may reflect a range of cell types, buffer composition, buffer pH, subunit composition, and the concentration of GABA used. In particular, these histidine residues are close to their pK_a,[29] so that a small change in buffer pH could produce a large change in Zn^{2+} affinity. The close agreement between our modeling and experimental data support the suggestion that pore-lining histidine residues in the $GABA_A$-R pore are not protonated at physiological pH.[29] The dramatic decrease in affinity observed for Zn^{2+} in $GABA_A$-R is consistent with the loss of affinity for Zn^{2+} and Cu^{2+} in other well-characterized sites, in which one histidine has been removed from a bidentate metal ion-binding site.[26,30,31]

Several site directed mutagenesis studies of the extracellular end of LGIC TM2 α helices have demonstrated that this region of the receptor plays a pivotal role in channel gating[32,33] and channel modulation.[21] All of these studies stressed the important role individual subunits play in receptor function. However, a critical component of LGIC activation is the interaction between adjacent subunits in binding ligands and the resulting relative motions between neighboring subunits.[34,35] The results of the present study also demonstrate that neighboring TM2 segments can combine together in the presence of Zn^{2+} to either destabilize an open state or prolong one or more closed states. This type of mechanism is consistent with two important studies: Zn^{2+} inhibition of current through the $GABA_A$-R is independent of membrane potential[8] suggesting that the mechanism is allosteric in nature and despite being close to the channel lumen, it is not due to channel blockade.[36]

It is noteworthy that hydration of our model of $\alpha1\beta2$ $GABA_A$-R plus Zn^{2+} resulted in the replacement of a histidine or glutamate by one or two water molecules. This result is consistent with a prediction by Valee and Auld in the "Velcro mechanism" for the activation of matrix prometalloproteinases.[37] Although a T4 tetrahedral coordination geometry for Zn^{2+} is common, a review of Zn^{2+} sites in a variety of crystal structures also revealed T5 square pyramidal, T5 trigonal bipyrimidal, and T6 octahedral geometries.[25] The capacity of Zn^{2+} to adopt different coordination geometries is also consistent with our finding that, at 300 K in molecular dynamics simulations, the binding of Zn^{2+} is fluid and several final configurations are possible.

The computational models and site-directed mutations confirm previous experimental evidence for involvement of pore-lining histidine residues in Zn^{2+} inhibition.[12] In a sense, our paradigm is the mirror image of that used by Hosie et al. to reach the same conclusion; they subtracted histidine and glutamate residues from a $\beta3$ subunit in $\alpha1\beta3$ $GABA_A$-

R, whereas we inserted the corresponding residues into a $\gamma 2$ subunit in $\alpha 1\beta 2\gamma 2$ $GABA_A$-R. Our results also provide an explanation for a previous study in which exchanging only the 17′ Ile for His in the γ subunit of $\alpha 1\beta 2\gamma 2$ $GABA_A$-R was not sufficient to reinstate high affinity Zn^{2+} binding.[15] Our new finding, predicted by molecular modeling and confirmed by mutagenesis, is that the positively charged 20′ lysine side chain of a $\gamma 2$ subunit can disrupt Zn^{2+} by interacting with neighboring negatively charged side chains. The combined results provide additional evidence for the involvement of the 20′ glutamate residue in the $GABA_A$-R β subunit in the formation of a tetradentate binding site for Zn^{2+}.

ACKNOWLEDGMENT

This research was supported by grants from the National Institutes of Health: NIAAA (AA13378 (to J.R.T. and E.B.), AA 16393 and AA 13646 (to N.L.H.), NIGMS GM073959 (to A.J.), and the Veterans Administration (to E.B.).

REFERENCES AND NOTES

(1) Nagaya, N.; MacDonald, R. L. Two gamma2L subunit domains confer low Zn2+ sensitivity to ternary GABA(A) receptors. *J. Physiol.* **2001**, *532*, 17−30.
(2) McKernan, R. M.; Whiting, P. J. Which GABAA-receptor subtypes really occur in the brain? *Trends Neurosci.* **1996**, *19*, 139−143.
(3) Farrant, M.; Nusser, Z. Variations on an inhibitory theme: phasic and tonic activation of GABA(A) receptors. *Nat. Rev. Neurosci.* **2005**, *6*, 215−229.
(4) Ernst, M.; Bruckner, S.; Boresch, S.; Sieghart, W. Comparative models of GABAA receptor extracellular and transmembrane domains: Important insights in pharmacology and function. *Mol. Pharmacol.* **2005**, *68*, 1291−1300.
(5) Harrison, N. L.; Gibbons, S. J. Zn2+: an endogenous modulator of ligand- and voltage-gated ion channels. *Neuropharmacology* **1994**, *33*, 935−952.
(6) Frederickson, C. J.; Koh, J. Y.; Bush, A. I. The neurobiology of zinc in health and disease. *Nat. Rev. Neurosci.* **2005**, *6*, 449−462.
(7) Kodirov, S. A.; Takizawa, S.; Joseph, J.; Kandel, E. R.; Shumyatsky, G. P.; Bolshakov, V. Y. Synaptically released zinc gates long-term potentiation in fear conditioning pathways. *Proc. Natl. Acad. Sci. U.S.A.* **2006**, *103*, 15218−15223.
(8) Westbrook, G. L.; Mayer, M. L. Micromolar concentrations of Zn2+ antagonize NMDA and GABA responses of hippocampal neurons. *Nature* **1987**, *328*, 640−643.
(9) Draguhn, A.; Verdorn, T. A.; Ewert, M.; Seeburg, P. H.; Sakmann, B. Functional and molecular distinction between recombinant rat GABAA receptor subtypes by Zn2+. *Neuron* **1990**, *5*, 781−788.
(10) Smart, T. G.; Moss, S. J.; Xie, X.; Huganir, R. L. GABAA receptors are differentially sensitive to zinc: dependence on subunit composition. *Br. J. Pharmacol.* **1991**, *103*, 1837−1839.
(11) Gingrich, K. J.; Burkat, P. M. Zn2+ inhibition of recombinant GABAA receptors: an allosteric, state-dependent mechanism determined by the gamma-subunit. *J. Physiol.* **1998**, *506*, 609−625.
(12) Hosie, A. M.; Dunne, E. L.; Harvey, R. J.; Smart, T. G. Zinc-mediated inhibition of GABA(A) receptors: discrete binding sites underlie subtype specificity. *Nat. Neurosci.* **2003**, *6*, 362−369.
(13) Hall, A. C.; Stevens, R. J.; Betts, B. A.; Yeung, W. Y.; Kelley, J. C.; Harrison, N. L. Subunit-dependent block by isoflurane of wild-type and mutant alpha(1)S270H GABA(A) receptor currents in Xenopus oocytes. *Neurosci. Lett.* **2005**, *382*, 332−337.
(14) Wooltorton, J. R.; McDonald, B. J.; Moss, S. J.; Smart, T. G. Identification of a Zn2+ binding site on the murine GABAA receptor complex: dependence on the second transmembrane domain of beta subunits. *J. Physiol.* **1997**, *505*, 633−640.
(15) Horenstein, J.; Akabas, M. H. Location of a high affinity Zn2+ binding site in the channel of alpha1beta1 gamma-aminobutyric acidA receptors. *Mol. Pharmacol.* **1998**, *53*, 870−877.
(16) Bertaccini, E.; Trudell, J. R. Predicting the transmembrane secondary structure of ligand-gated ion channels. *Protein Eng.* **2002**, *15*, 443−453.
(17) Trudell, J. R.; Bertaccini, E. Comparative modeling of a GABAA a1 receptor using three crystal structures as templates. *J. Mol. Graphics Modell.* **2004**, *23*, 39−49.
(18) Bertaccini, E.; Shapiro, J.; Brutlag, D.; Trudell, J. R. Homology modeling of a human glycine alpha 1 receptor reveals a plausible anesthetic binding site. *J. Chem. Inf. Model.* **2005**, *45*, 128−135.
(19) Unwin, N. Refined structure of the nicotinic acetylcholine receptor at 4A resolution. *J. Mol. Biol.* **2005**, *346*, 967−989.
(20) Campagna-Slater, V.; Weaver, D. F. Molecular modelling of the GABAA ion channel protein. *J. Mol. Graphics Modell.* **2007**, *25*, 721−730.
(21) Mihic, S. J.; Ye, Q.; Wick, M. J.; Koltchine, V. V.; Krasowski, M. D.; Finn, S. E.; Mascia, M. P.; Valenzuela, C. F.; Hanson, K. K.; Greenblatt, E. P.; Harris, R. A.; Harrison, N. L. Sites of alcohol and volatile anaesthetic action on GABA(A) and glycine receptors. *Nature* **1997**, *389*, 385−389.
(22) Paas, Y.; Gibor, G.; Grailhe, R.; Savatier-Duclert, N.; Dufresne, V.; Sunesen, M.; de Carvalho, L. P.; Changeux, J. P.; Attali, B. Pore conformations and gating mechanism of a Cys-loop receptor. *Proc. Natl. Acad. Sci. U.S.A.* **2005**, *102*, 15877−15882.
(23) Brejc, K.; van Dijk, W. J.; Klaassen, R. V.; Schuurmans, M.; van Der, O. J.; Smit, A. B.; Sixma, T. K. Crystal structure of an ACh-binding protein reveals the ligand-binding domain of nicotinic receptors. *Nature* **2001**, *411*, 269−276.
(24) Miyazawa, A.; Fujiyoshi, Y.; Unwin, N. Structure and gating mechanism of the acetylcholine receptor pore. *Nature* **2003**, *423*, 949−955.
(25) Alberts, I. L.; Nadassy, K.; Wodak, S. J. Analysis of zinc binding sites in protein crystal structures. *Protein Sci.* **1998**, *7*, 1700−1716.
(26) Higaki, J. N.; Fletterick, R. J.; Craik, C. S. Engineered metalloregulation in enzymes. *Trends Biochem. Sci.* **1992**, *17*, 100−104.
(27) Trudell, J. R. Unique assignment of inter-subunit association in GABAa alpha1 beta3 gamma2 receptors determined by molecular modeling. *Biochim. Biophys. Acta* **2002**, *1565*, 91−96.
(28) Cromer, B. A.; Morton, C. J.; Parker, M. W. Anxiety over GABA(A) receptor structure relieved by AChBP. *Trends Biochem. Sci.* **2002**, *27*, 280−287.
(29) Cymes, G. D.; Ni, Y.; Grosman, C. Probing ion-channel pores one proton at a time. *Nature* **2005**, *438*, 975−980.
(30) Norregaard, L.; Visiers, I.; Loland, C. J.; Ballesteros, J.; Weinstein, H.; Gether, U. Structural probing of a microdomain in the dopamine transporter by engineering of artificial Zn(2+) binding sites. *Biochemistry* **2000**, *39*, 15836−15846.
(31) Venkataraman, P.; Lamb, R. A.; Pinto, L. H. Chemical rescue of histidine selectivity filter mutants of the M2 ion channel of influenza A virus. *J. Biol. Chem.* **2005**, *280*, 21463−21472.
(32) Koltchine, V. V.; Finn, S. E.; Jenkins, A.; Nikolaeva, N.; Lin, A.; Harrison, N. L. Agonist gating and isoflurane potentiation in the human gamma- aminobutyric acid type A receptor determined by the volume of a second transmembrane domain residue. *Mol. Pharmacol.* **1999**, *56*, 1087−1093.
(33) Nishikawa, K.; Jenkins, A.; Paraskevakis, I.; Harrison, N. L. Volatile anesthetic actions on the GABA(A) receptors: contrasting effects of alpha1(S270) and beta2(N265) point mutations. *Neuropharmacology* **2002**, *42*, 337−345.
(34) Bertaccini, E.; Trudell, J. R.; Lindahl, E. Normal mode analysis reveals the channel gating motion within a ligand gated ion channel model. *Int. Cong. Ser.* **2005**, *1283*, 160−163.
(35) Bertaccini, E. J.; Lindahl, E.; Trudell, J. R. Normal mode analysis of the Glycine alpha 1 receptor by three separate methods. *J. Chem. Inf. Model.* **2007**, *47*, 1572−1579.
(36) White, G.; Gurley, D. A. Alpha subunits influence Zn block of gamma 2 containing GABAA receptor currents. *Neuroreport* **1995**, *6*, 461−464.
(37) Vallee, B. L.; Auld, D. S. Zinc coordination, function, and structure of zinc enzymes and other proteins. *Biochemistry* **1990**, *29*, 5647−5659.

CI700324A